Biomaterials and Biomechanics in Bioengineering, *Vol. 4, No. 1 (2019) 45-58*
DOI: https://doi.org/10.12989/bme.2019.4.1.045

Analysis of the size-dependent wave propagation of a single lamellae based on the nonlocal strain gradient theory

Farzad Ebrahimi[*1], Farin Zokaee[1] and Vinyas Mahesh[2]

[1]*Faculty of engineering, Imam Khomeini International University, Qazvin, Iran*
[2]*Department of Mechanical Engineering, Nitte Meenakshi Institute of Technology, Bangalore, India*

(Received January 14, 2019, Revised Marh 20, 2019, Accepted March 21, 2019)

Abstract. In the present article, the general wave propagation behavior of a single lamellae biological system was analyzed. The Lamellae is the main component of cortical bone. Its shape can be approximated by a cylindrical shell; so with using shell theories as displacement relations and the nonlocal strain gradient theory (NSGT) as constitutive relation was obtained the equation of motion. Using the NSGT leads to the effectiveness of scale parameter on equations of motion and the obtained results. The governing equations are derived by Hamilton's principles. The results are showing the variations of the overall trend of wave velocity toward wave vector have descending scheme and wave frequency against wave vector have ascending scheme; also were investigated effects of size and geometrical parameters on wave velocity and wave frequency. It was shown uptrend of types of wave velocities for wave vectors greater than 10^5.

Keywords: bone; lamellae, osteon; wave propagation; size effect

1. Introduction

Surveying biological material from the perspective of engineering science extremely has been done to achieve: a) biomimetic material, b) displaying vital signs status c) improve functionality and elimination of defects of living organs; in the simple word, investigators are trying to incept from which be and optimized during millions of years or trying to show what those are, or trying to add something to biological structures to make a more optimized system. Mathematical analysis of biological structures has always been a favorite of researchers; as a better understanding of these structures and more importantly, it is possible to predict their behavior in different situations.

Bone as a biological structure is the solid compound of the skeleton of creatures and the part of the framework of the body, among duties of this member is, making strength in the body, protection of some tissues, etc. Bones are the place for the production of white blood cells and red blood cells. They are a source of minerals, in particular, calcium; bones transmit minerals whenever the body needs them. Most bones are composed of two parts: a) spongy bone, b) cortical bone. The outer part (cortical bone) of the rigid bone is made of collagen and calcium structure as hydroxyapatite and so on. However, there are other tissues such as blood vessel and nerve in it. This section of bones are made of units with the regular arrangement are known as the Haversian

∗Corresponding author, Associate Professor, E-mail: febrahimy@eng.ikiu.ac.ir

http://www.techno-press.org/?journal=bme&subpage=8 ISSN: 2465-9835 (Print), 2465-9959 (Online)

system. Haversian system consists of a central hole (Havers's duct) that contains the nerves and vessels and bony centered cylinders that are called lamellae which surrounds the central hole. Every 5-6 lamellae make the osteon unit (Cowin and Stephen 2001). Done works on this structure, in the past, are as below: Rho *et al.* in 1998 surveyed the entire mechanical works done on the bone before and finally with asking some questions delivered the work to others. Liu *et al.* (1999) carried out experiments on the lamellae and extruded flexural module and work-to-fatigue of it. Gourion-Arsiquaud *et al.* (2014) studied the structure of bone with a scanning electron microscope (SEM) and transmission electron microscope (TEM) and obtained young modules, flexural modules and work-to-fatigue of lamellae.

Hoffler *et al*. (2000) performed nanoindentation test and achieved to mechanical properties of bone such hardness and elastic moduli. Sun *et al*. (2016) studied the mechanical properties of lamellae in the various plane. Hassenkam *et al.* (2004) performed tests to obtain the mechanical properties of bone with focus approach on the nanostructure of bone. Currey *et al.* (2006) extracted coefficients of variation of mechanical properties of bone; and then also they (Currey and John 2011) investigated the hierarchal structure of bone. Faingold *et al*. (2013) with nanoindentation and SEM surveyed properties of single lamellae in various plates. Ren *et al.* (2015) studied various aspects of mechanical properties of bone such as the hierarchical structure of bone and fluid flow in bone and hydrostatic pressure. Also Wang *et al.* (2018) presented a pin-moment model of flexoelectric actuators while active vibration compensator on moving vessel by hydraulic parallel mechanism was investigated by Tanaka (2018).

Weiner *et al*. (1999) investigated the components of bone with Atomic force microscope infrared (AFM-IR) test and Fourier-Transform Infrared (FTIR) spectroscopy. Mitchell *et al.* (2015) for a better understanding of lamellae investigated the arrangement of the fiber of lamellae, thickness, orientation, and its compositions. Xie *et al*. (2017) studied time-dependent properties of bone and dependence of those to volume fraction. Unal *et al.* (2018) investigated hygro- electrical properties of bone. Hamed *et al.* (2010) modeled cortical bone as composite material and hierarchical levels and extracted elastic moduli and stiffness matrix of cortical bone; as an extension, they carried out the same work with continuum approach and finite element and achieved to good agreement with experimental results (Hamed *et al*. 2012).

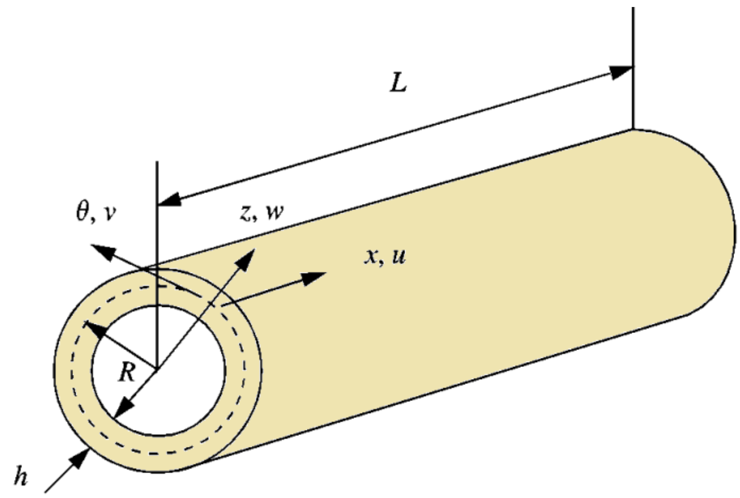

Fig. 1 Shape of a single lamellae with showing angular coordinate system elements

However, even though the mechanics of the bone belongs to bioengineering, at the nano range it can be mapped to nano mechanical structures to understand its stability and other mechanical responses. Few prominent kinds of literature have been reported on assessing the various characteristics of nanoplates and nanobeams. Among them, Tlidji *et al.* (2019) evaluated the free vibration response of FG microbeam. Through refined nonlocal shear deformation beam theory, Zemri *et al.* (2015) investigated the mechanical response of FG nanobeams. Bouafia *et al.* (2017) probed the bending and free flexural vibration behaviors of functionally graded nanobeams using A nonlocal quasi-3D theory. Considering the surface effects, the dynamic behaviour of nanobeams were studied by Youcef *et al.* (2018). The effect of thermal environment on the vibration analysis of nano and micro beam were performed by Cherif *et al.* (2018), Akgoz and Civalek (2017), Ebrahimi and Salari (2015). Using new nonlocal trigonometric shear deformation theory, the free vibration analysis of embedded nanosize FG plates was studied by Besseghier *et al.* (2017). It was extended by Mouffoki *et al.* (2017) to demonstrate the influence of hygrothermal effects on the natural frequencies. Also, other elasticity theories are proved to be handy in assessing the dynamic characteristics of nanostructures (Shaat 2018).

With the externally applied loading, the stability analysis of nanostructures becomes crucial to understand. In this regard, Yazid *et al*. (2018) proposed a new nonlocal higher order shear deformation theory and nonlocal refined plate theory, respectively to evaluate the stability response of single-layer graphene sheet. Mercan and Civalek (2016) demonstrated the buckling response of boron nitride nanotube through DSC method and extended their evaluation for Silicon carbide nanotubes (SiCNTs). Bellifa *et al.* (2017) studied the nonlinear post-buckling behaviour of nanobeams through nonlocal zeroth-order shear deformation theory. Based on nonlocal elasticity theory, Mokhtar *et al.* (2018), studied the buckling analysis of single-layer graphene sheet. The buckling analysis of various nanostructures in the thermal environment was also studied and reported in the literature (Ebrahimi *et al.* 206 a,b, Ebrahimi and Salari 2015a, b). The prominence of elastic foundations and neutral surface position concept in assessing the mechanical behaviour of nanostructures were also highlighted (Ebrahimi and Barati 2016f-n, Ebrahimi and Barati 2017, Larbi Chaht *et al*. 2015).

Despite the fact that Eringen's nonlocal theory is broadly applied to take into consideration of the small scale effects, it considers only the stiffness-softening influence. It is reported that the nonlocal elasticity theory is unable to predict the stiffness-hardening effects by introducing the length scale parameter. In the nonlocal strain gradient theory, the stress field accounts for not only the nonlocal stress field but also the strain gradients stress field (Karami *et al*. 2018).

As mentioned before the cortical bone has a hierarchical structure and composed from units have been called osteon. An osteon composed of 5-6 cylindrical shells that have been called lamellae. In this paper, for the first time, employed an analytical method for better understanding of behavior of bone and analyzed wave propagation of a single lamellae with considering size effect by NSGT and governing equations of lamellae derived by using Hamilton's principle.

2. Mechanical model

The single lamellae can be modeled as a hollow cylindrical shell (Fig. 1). In the present paper the NSGT is used for modeling lamellae (Yazid *et al.* 2018). The stiffness matrix of a single lamellae which is obtained experimentally, is as below Sun *et al*. (2016)

$$C(GPa)=\begin{bmatrix}16.08 & 6.21 & 0\\ 6.22 & 16.07 & 0\\ 0 & 0 & 9.88\end{bmatrix} \tag{1}$$

The lamellae displacement fields are denoted by *U*, *V*, and *W* in *x*, θ, and *z* coordinates. The values of these displacements based on the love thin shell theory can express as below

$$U=u_0-zw_{,x}$$

$$V=v_0-(z/R)(w_{,\theta}-v_0) \tag{2}$$

$$W=w_0$$

where u_0, v_0, w_0 are axial, circumferential, and radial displacements, respectively. In these equations, has been called radius by *R*, thickness by h and mass density by ρ. We use *x*, θ and *z* as angular coordinate elements, perpendicular to the lamellae axis The strain components ε_x, ε_θ, $\gamma_{x\Theta}$ $\gamma_{x\Theta}$ at an arbitrary point of the shell, are as below

$$\varepsilon_x=u_{,x}-zw_{,xx} \tag{3}$$

$$\varepsilon_\theta=\frac{v_{,\theta}+w}{R}-\frac{z}{R^2}\frac{\partial^2 w}{\partial\theta^2} \tag{4}$$

$$\gamma_{x\theta}=\frac{1}{2}\left[\frac{u_{,\theta}}{R}+v_{,x}-2z\frac{w_{,x\theta}}{R}\right] \tag{5}$$

The stress-strain relationships based on NSGT can be written as

$$\sigma_{ij}=(1-(l_s)^2\nabla^2)C_{ijkl}\varepsilon_{kl} \tag{6}$$

And for using Hamilton's principle we need to obtain strain energy U, kinetic energy K and work of external forces W

$$\int_0^t \delta(U-T+W)dt=0 \tag{7}$$

Strain energy U of lamellae is expressed as below

$$U=\frac{1}{2}\int_\forall \sigma_{ij}\varepsilon_{kl}\,d\forall \tag{8}$$

$$\delta U=\frac{1}{2}\iiint_V(\sigma_{ij}\delta\varepsilon_{ij})dV=\iint_A A\left\{\begin{array}{l}(N_{xx}\frac{\partial}{\partial x}\delta u+M_{xx}\frac{\partial^2}{\partial x^2}\delta W)+N_{\theta\theta}(\frac{1}{R}\frac{\partial}{\partial\theta}\delta v+\frac{\delta w}{R})+\\ M_{\theta\theta}\frac{1}{R^2}\frac{\partial^2}{\partial\theta^2}\delta W+\\ N_{x\theta}(\frac{1}{R}\frac{\partial}{\partial\theta}\delta u+\frac{\partial}{\partial x}\delta v)-2M_{x\theta}(\frac{\partial^2}{\partial x\partial\theta}\delta W)\end{array}\right\}Rdxd\theta \tag{9}$$

where in that

$M_{ij}= \int_{-h/2}^{h/2} z\sigma_{ij}\, dz$

$N_{ij} = \int_{-h/2}^{h/2} \sigma_{ij}\, dz$

$A = (1-(l_s)^2\nabla^2)$

and for kinetic energy K we have

$$T = \frac{1}{2}\rho\int_V (\dot{u}^2 + \dot{v}^2 + \dot{w}^2)dV \tag{10}$$

$$\delta T = \rho\int_V (\dot{u}\delta\dot{u} + \dot{v}\,\delta\dot{v} + \dot{w}\,\delta\dot{w})dV \tag{11}$$

and then we have

$$\delta T = \rho\int_x\int_\theta [\ hR\left(\frac{\partial^2 w}{\partial t^2}\right)\delta w + hR\left(\frac{\partial^2 u}{\partial t^2}\right)\delta u + hR\left(\frac{\partial^2 v}{\partial t^2}\right)\delta v\ ]dx\,d\,\Theta \tag{12}$$

which with substitution

$$I_0 = \rho h \tag{13}$$

Eq. (12) become

$$\delta T = \rho\int_A [I_0 R\left(\frac{\partial^2 w}{\partial t^2}\right)\delta w + I_0 R\left(\frac{\partial^2 u}{\partial t^2}\right)\delta u + I_0 R\left(\frac{\partial^2 v}{\partial t^2}\right)\delta v\ ]dA \tag{14}$$

and for external forces we have

$$\delta W = \int (f_u\delta u + f_v\,\delta v + f_w\,\delta w)dA \tag{15}$$

By substituting Eqs. (9), (14), (15) into (7) and integrating by parts, equations of motion can be written as below

$$\begin{aligned}
&\delta u : \left\{A_{11}\frac{\partial^2 u}{\partial x^2} + A_{12}\left(\frac{\partial^2 v}{R\partial x\,\partial\theta} + \frac{1}{R}\frac{\partial w}{\partial x}\right)\right\} + \\
&\frac{1}{R}\left\{A_{33}\left(\frac{1}{R}\frac{\partial^2 u}{\partial^2\theta} + \frac{\partial^2 v}{\partial x\,\partial\theta}\right)\right\} - \\
&\frac{1}{2R^2}\left\{-A_{44}l^2\left[\frac{1}{R}\left(\frac{1}{R}\frac{\partial^2 u}{\partial\,\theta^2} - \frac{\partial^2 v}{\partial x\,\partial\theta}\right) + \frac{1}{R}\frac{\partial^3 w}{\partial x\,\partial\theta^2}\right]\right\} + \\
&\frac{1}{2R^2}\left\{-A_{44}l^2\left[-\frac{1}{R^2}\frac{\partial^2 u}{\partial\theta^2}\right]\right\} + \\
&\frac{1}{2R}\left\{-\frac{A_{44}l^2}{2}\left[-\frac{\partial^4 v}{\partial x^3\partial\theta} - \frac{1}{R^2}\frac{\partial^2 v}{\partial\theta\,\partial x} + \frac{1}{R}\frac{\partial^4 u}{\partial x^2\partial\theta^2} + \frac{1}{R^2}\frac{\partial^3 w}{\partial x\,\partial\theta^2}\right]\right\} + \\
&\frac{1}{2R^2}\frac{\partial^2}{\partial\theta^2}\left\{-\frac{A_{44}l^2}{2}\left[\frac{1}{R^2}\frac{\partial^4 u}{\partial\theta^4} - \frac{1}{R}\frac{\partial^4 v}{\partial x\,\partial\theta^3} - \frac{1}{R}\frac{\partial^3 w}{\partial x\,\partial\theta^2}\right]\right\} = I_0\frac{\partial^2 u}{\partial t^2} + f_u
\end{aligned} \tag{16}$$

$$
\begin{aligned}
&\delta v :\left\{A_{33}\left(\frac{1}{R}\frac{\partial^2 u}{\partial x\,\partial\theta}+\frac{\partial^2 v}{\partial x^2}\right)\right\}+\\
&\frac{1}{R}\left\{A_{11}\left(\frac{1}{R}\frac{\partial w}{\partial\theta}+\frac{1}{R}\frac{\partial^2 v}{\partial\theta^2}\right)+A_{12}\frac{\partial^2 u}{\partial\theta\partial x}\right\}\\
&-\frac{1}{2R}\left\{-A_{44}l^2\left(\frac{1}{R}\frac{\partial^2 v}{\partial x^2}-\frac{1}{R}\frac{\partial^3 w}{\partial x^2\partial\theta}\right)\right\}+\frac{1}{2R}\frac{\partial}{\partial x}\left\{-A_{44}l^2\left[\frac{1}{R}\left(\frac{1}{R}\frac{\partial^2 u}{\partial x\,\partial\theta}-\frac{\partial^2 v}{\partial x^2}\right)+\frac{1}{R}\frac{\partial^3 w}{\partial x^2\partial\theta}\right]\right\}\\
&-\frac{1}{R^2}\left\{-\frac{A_{44}l^2}{4}\left(\frac{1}{R^2}\frac{\partial^2 v}{\partial^2\theta}+\frac{\partial^3 w}{\partial x^2\partial\theta}-\frac{1}{R^2}\frac{\partial^3 w}{\partial\theta^3}\right)\right\}\\
&-\left\{-\frac{A_{44}l^2}{4}\left[-\frac{\partial^4 v}{\partial x^4}-\frac{1}{R^2}\frac{\partial^2 v}{\partial x^2}+\frac{1}{R}\frac{\partial^4 u}{\partial x^3\partial\theta}+\frac{1}{R^2}\frac{\partial^3 w}{\partial x^2\partial\theta}\right]\right\}\\
&-\frac{1}{R^2}\left\{-\frac{A_{44}l^2}{4}\left[-\frac{\partial^2 v}{\partial x^2}-\frac{v}{R^2}+\frac{1}{R}\frac{\partial^2 u}{\partial x\,\partial\theta}+\frac{1}{R^2}\frac{\partial w}{\partial\theta}\right]\right\}\\
&-\frac{1}{R}\left\{-\frac{A_{44}l^2}{4}\left[\frac{1}{R^2}\frac{\partial^4 u}{\partial\theta^3\partial x}-\frac{1}{R}\frac{\partial^4 v}{\partial x^2\partial\theta^2}-\frac{1}{R}\frac{\partial^3 w}{\partial x^2\partial\theta}\right]\right\}=I_0\frac{\partial^2 v}{\partial t^2}+f_v
\end{aligned}
\tag{17}
$$

$$
\begin{aligned}
&\delta w :-\frac{1}{R}\left\{A_{11}\left(\frac{w}{R}+\frac{1}{R}\frac{\partial v}{\partial\theta}\right)+A_{12}\frac{\partial u}{\partial x}\right\}-\\
&\frac{1}{2R^2}\left\{-\frac{A_{44}l^2}{2}\left(\frac{1}{R^2}\frac{\partial^3 v}{\partial\theta^3}+\frac{\partial^4 w}{\partial x^2\partial\theta^2}-\frac{1}{R^2}\frac{\partial^4 w}{\partial\theta^4}\right)\right\}-\\
&\frac{1}{2R^2}\left\{-\frac{A_{44}l^2}{2}\left[-\frac{\partial^3 v}{\partial x^2\partial\theta}-\frac{1}{R^2}\frac{\partial v}{\partial\theta}+\frac{1}{R}\frac{\partial^3 u}{\partial x\,\partial\theta^2}+\frac{1}{R^2}\frac{\partial^2 w}{\partial\theta^2}\right]\right\}+\\
&\frac{1}{2R}\left\{-\frac{A_{44}l^2}{2}\left[\frac{1}{R^2}\frac{\partial^3 u}{\partial x\,\partial\theta^2}-\frac{1}{R}\frac{\partial^3 v}{\partial x^2\partial\theta}-\frac{1}{R}\frac{\partial^2 w}{\partial x^2}\right]\right\}+\\
&\frac{1}{2}\left\{-\frac{A_{44}l^2}{2}\left(\frac{1}{R^2}\frac{\partial^3 v}{\partial x^2\partial\theta}+\frac{\partial^4 w}{\partial x^4}-\frac{1}{R^2}\frac{\partial^4 w}{\partial x^2\partial\theta^2}\right)\right\}\\
&-\frac{1}{2R}\left\{-A_{44}l^2\left(\frac{1}{R}\frac{\partial^3 v}{\partial x^2\partial\theta}-\frac{1}{R}\frac{\partial^4 w}{\partial x^2\partial\theta^2}\right)\right\}+\\
&\frac{1}{2R}\left\{-A_{44}l^2\left[\frac{1}{R}\left(\frac{1}{R}\frac{\partial^3 u}{\partial\theta^2\partial x}-\frac{\partial^3 v}{\partial\theta\partial x^2}\right)+\frac{1}{R}\frac{\partial^4 w}{\partial x^2\partial\theta^2}\right]\right\}=I_0\left(\frac{\partial^2 w}{\partial t^2}\right)+f_w
\end{aligned}
\tag{18}
$$

which in those the parameters are

$$\{A_{11}\}=\int_{-h/2}^{h/2}c_{11}dz\,,\qquad \{A_{12}\}=\int_{-h/2}^{h/2}c_{12}dz\,,$$

$$\{A_{33}\}=\int_{-h/2}^{h/2}c_{66}dz\,,\qquad \{A_{44}\}=\int_{-h/2}^{h/2}\mu dz\,,$$

$$\mu=(e_0a/l)^2$$

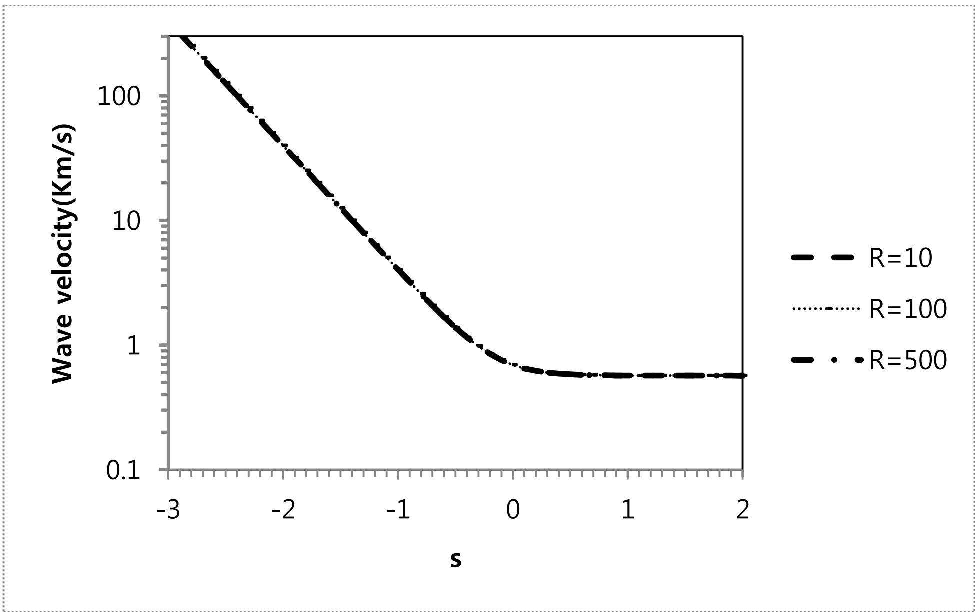

Fig. 2 Variation of wave velocity in different R of the lamellae, with n=1, l_s=1nm, h=1nm

3. Solution method

For non-axisymmetric waves which in that n>0, the solution of wave given by

$$
\begin{aligned}
u &= U \sin k_x (x - ct).\cos(n\theta) \\
v &= V \cos k_x (x - ct).\sin(n\theta) \\
w &= W \cos k_x (x - ct).\cos(n\theta)
\end{aligned} \tag{19}
$$

where U, V and W are an undefined constant of amplitude in the longitudinal, circumferential and radial directions, c is the wave velocity and k_x is the wave vector in the longitudinal direction. Substituting Eq. (19) in Eqs. (16)-(18), leads to three coupled equations that can be written as

$$
\begin{bmatrix} F_{11} & F_{12} & F_{13} \\ F_{21} & F_{22} & F_{23} \\ F_{31} & F_{32} & F_{33} \end{bmatrix} . \begin{bmatrix} U \\ V \\ W \end{bmatrix} = 0 \tag{20}
$$

where in that, F_{ij} is functions of k_x, c and n. since matrix $\begin{bmatrix} U \\ V \\ W \end{bmatrix}$ can't be equal to zero, then the determinant of the following matrix should be equal to zero

$$\det\begin{bmatrix} F_{11} & F_{12} & F_{13} \\ F_{21} & F_{22} & F_{23} \\ F_{31} & F_{32} & F_{33} \end{bmatrix} = 0 \tag{21}$$

with considering $K=k_x/R$ and $K=10^s$, with knowing n we can obtain c. In addition, Eigen values of this matrix give the natural frequency.

4. Result and discussion

As the importance of bone in the structure of the body, investigation of wave propagation of component of this vital member was investigated. Those components of cortical bone include of osteons, lamellae and so on. In this paper, the single lamellae's wave propagation characteristic has been studied for a different set of parameters. The component of stiffness matrix was presented in Eq. (1). In this case density ρ was considered 49850 and radius of lamellas R vary from 10 to 500 micrometer, the thickness of lamellas h varies from 1 to 10 micrometer. For the sake of comparison, the respect between wave vector and wave velocity and wave frequency, shown in figures.

First, we examine the ratio of varying longitudinal wave velocity compared to varying wave vector with considering a various radius of a single lamellae, with n=1, l_s=1*10^-9, and thickness h=1 nanometer; it can be seen as shown in the Fig. 2 that radius changes don’t have effects on wave velocity. In Fig. 3 we compared the natural frequency toward wave vector; we showed shade in the charts of the different radius in lower wave vector but in higher wave vector the radius has an insensitive effect on wave frequency of a lamellae.

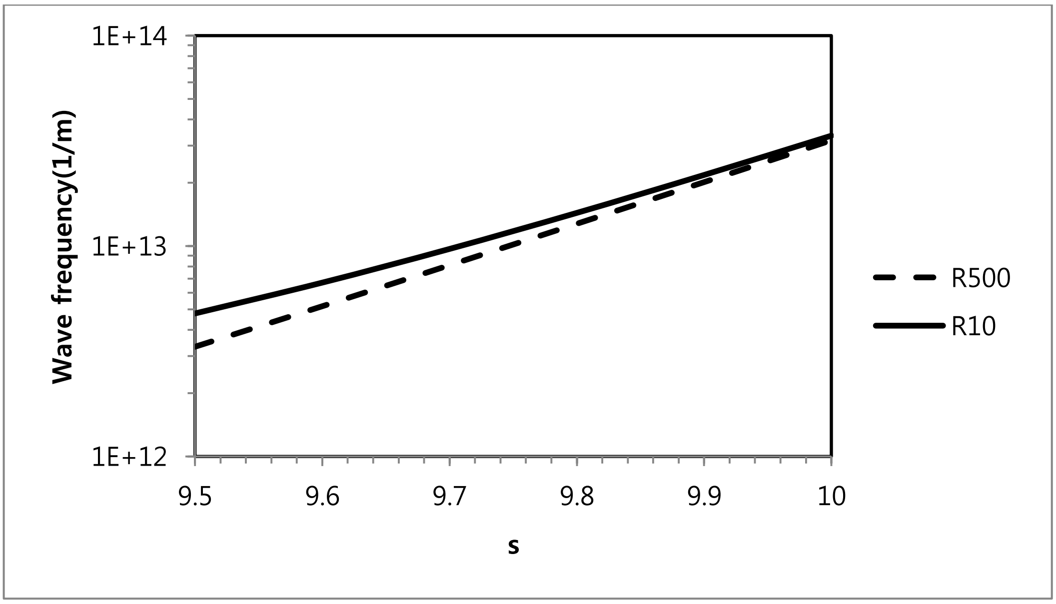

Fig. 3 Variation of longitudinal wave frequency in different R of the lamella, with n=1, ls=1nm, h=1nm

Table2 Variation of wave frequency toward n of a lamellae, with R=100 nm, h=1 nm, l_s=1 nm

s	Wave frequency(1/nm)		
	n=1	n=5	n=10
0	5.2334	5.23796	5.23804
0.5	16.4065	16.5598	16.5598
1	44.669	52.2075	52.2075
1.5	120.653	147.515	147.515
2	454.585	3229.01	3229.01
2.5	3323.63	4458.27	5385.76
3	31801.6	33051.6	36559.6
3.5	316510	317816	321601

Table 3 variation in longitudinal wave velocity toward variation l_s of lamellae, with R=100 nm,n=1

s	Wave velocity(Km/s)		
	l_s(nm)		
	0	1	2
0	0.650129	0.650129	0.650129
0.5	0.576696	0.576696	0.576696
1	0.568831	0.568831	0.568831
1.5	0.568039	0.568039	0.568039
2	0.567959	0.56796	0.56796
2.5	0.567951	0.567954	0.567963
3	0.567951	0.567979	0.568064
3.5	0.56795	0.568234	0.569085
4	0.56795	0.570783	0.579198

In Fig. 4 has been shown the overall trend changes of longitudinal wave frequency of a lamellae while n=1, l_s=1 nm, and radius of lamellae is 100nm and its thickness is 1nm; Fig. 4 show when s>9 wave frequency has a very sharp uptrend. Also varying in wave frequencies with different circumferential wave number have been shown in Table 1; it is visible incremental effect of n on wave frequency in this table. Variation of longitudinal wave velocity with a variation of size effect coefficient is visible in Table 2; variation of radial wave velocity with a variation of size effect coefficient is visible in Table 3; variation of radial wave velocity with a variation of size effect coefficient is visible in Table 4. All three Tables 2-4 show the incremental rate of phase velocity commensurate with the size coefficient. Changes in wave frequencies with considering a variation of thickness h are visible in Fig. 5. It should be mentioned that these variations have a complicated but shading relationship with together; the most clear difference is relate to 8.5<s< 9.5 that as increasing in h wave velocities increased.

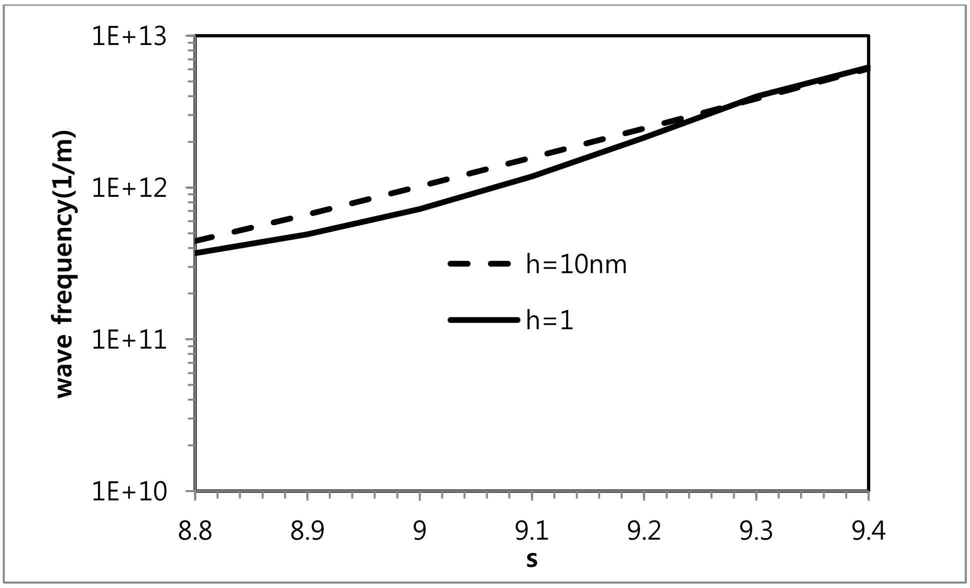

Fig. 5 Variation of wave frequency toward s(=log(K)), with n=1, l_s=3 nm and R=100 nm

Table 4 variation in radial wave velocity toward variation l_s of lamellae, with R=100 nm, n=1

s	Wave velocity(Km/s)		
	l_s(nm)		
	0	1	2
0	10366.1	10366.1	10366.1
0.5	3278.04	3278.04	3278.04
1	1036.61	1036.61	1036.61
1.5	327.804	327.804	327.804
2	103.661	103.661	103.661
2.5	32.7804	32.7806	32.7811
3	10.3661	10.3666	10.3682
3.5	3.27808	3.27972	3.28463
4	1.03777	1.04295	1.05833

Fig. 6 compared the longitudinal, radial and circumferential wave velocities in the different wave vector with considering circumferential wave number n=1 and size coefficient l_s=3 nm. In this figure uptrend longitudinal wave velocity for s>5 was observed while radial and circumferential wave velocity for s<5 have decreasing trend and for s>5 have an increasing trend.

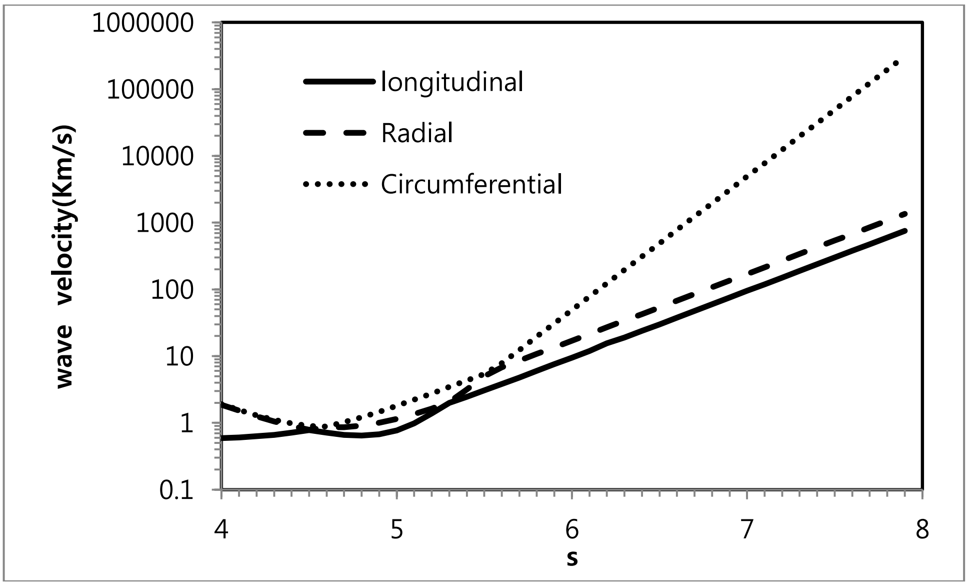

Fig. 6 Variation of wave velocity in different directions towards (=log(K)) , with n=1, l_s=3 nm

Table 5 Variation in circumferential wave velocity toward variation l_s of lamellae, with R=100 nm,n=1

s	Wave velocity(Km/s)		
	l_s(nm)		
	0	1	2
0	10366.1	10366.1	10366.1
0.5	3278.04	3278.04	3278.04
1	1036.61	1036.61	1036.61
1.5	327.805	327.805	327.805
2	103.661	103.661	103.662
2.5	32.782	32.7821	32.7826
3	10.3709	10.3714	10.373
3.5	3.29328	3.29492	3.29986
4	1.08382	1.08922	1.10528

5. Conclusions

In this article, a wave propagation characteristic of a single lamellae is explored using NSGT. To correlate with the structure of the bone, a beam model is adopted. Finally, with using some parametric study, the parameters such as radius, thickness, nonlocal coefficient, circumferential wave number on wave velocity and wave frequency of lamellae of bone are investigated. It is found that the variation in radius of lamellae does not have a significant effect on wave velocity but exhibit a shading effect on wave frequency. In addition it is observed that the size coefficient has an incremental effect on the wave velocity. Analogously, increase in the circumferential wave number improves the wave frequency. Effect of thickness on longitudinal wave frequency was seen just in the limited domain of wave vector. Comparison between types of wave velocities observed in a figure and was shown for s>5 all of them have incremental trend. It is believed that the results may act as benchmark solutions in the future analysis and evaluation of single lamellae.

References

Akgoz, B. and Civalek, O. (2017), "Effects of thermal and shear deformation on vibration response of functionally graded thick composite microbeams", *Compos. Part B: Eng.*, **129**, 77-87.

Bellifa, H., *et al*. (2017), "A nonlocal zeroth-order shear deformation theory for nonlinear postbuckling of nanobeams", *Struct. Eng. Mech.*, **62**(6), 695-702.

Besseghier, A., *et al*. (2017), "Free vibration analysis of embedded nanosize FG plates using a new nonlocal trigonometric shear deformation theory", *Smart Struct. Syst.*, **19**(6), 601- 614.

Bouafia, K., *et al.* (2017), "A nonlocal quasi-3D theory for bending and free flexural vibration behaviors of functionally graded nanobeams", *Smart Struct. Syst.*, **19**(2), 115-126.

Chaht, F.L., *et al.* (2015), "Bending and buckling analyses of functionally graded material (FGM) size-dependent nanoscale beams including the thickness stretching effect", *Steel Compos. Struct.*, **18**(2), 425-442.

Cowin, S. (2001), *Bone Mechanic Handbook*, Second edi, washengton DC, newyork: CRC.

Currey, J.D. (2011), "The structure and mechanics of bone", *Mater Sci*., **47**, 41-54.

Currey, J.D., Pitchford, J.W. and Baxterand, P.D. (2006), "Variability of the mechanical properties of bone, and its evolutionary consequences", *J. Royal Soc.*, **27**, 127-135.

Ebrahimi, F. and Salari, E. (2015a), "Thermo-mechanical vibration analysis of nonlocal temperature-dependent FG nanobeams with various boundary conditions", *Compos. Part B Eng*., **78**, 272-290.

Ebrahimi, F. and Salari, E. (2015b), "Thermal buckling and free vibration analysis of size dependent Timoshenko FG nanobeams in thermal environments", *Compos. Struct.*, **128**, 363-380.

Ebrahimi, F. and Salari, E. (2015c), "Size-dependent thermo-electrical buckling analysis of functionally graded piezoelectric nanobeams", *Smart Mater. Struct*., **24**(12),125007.

Ebrahimi, F. and Hosseini, S.H.S. (2016a), "Thermal effects on nonlinear vibration behavior of viscoelastic nanosize plates", *J. Therm. Stresses*, **39**(5), 606-625.

Ebrahimi, F. and Hosseini, S.H.S. (2016b), "Double nanoplate-based NEMS under hydrostatic and electrostatic actuations", *Eur. Phys. J. Plus*, **131**(5), 1-19.

Ebrahimi, F. and Barati, M.R. (2016f), "A nonlocal higher-order shear deformation beam theory for vibration analysis of size-dependent functionally graded nanobeams", *Arabian J. Sci. Eng*., **41**(5), 1679-1690.

Ebrahimi, F. and Barati, M.R. (2016g), "Vibration analysis of nonlocal beams made of functionally graded material in thermal environment", *Eur. Phys. J. Plus*, **131**(8), 279.

Ebrahimi, F. and Barati, M.R. (2016h), "Dynamic modeling of a thermo–piezo-electrically actuated nanosize beam subjected to a magnetic field", *Appl. Phys. A*, **122**(4), 1-18.

Ebrahimi, F. and Barati, M.R. (2016i), "A unified formulation for dynamic analysis of nonlocal heterogeneous nanobeams in hygro-thermal environment", *Appl. Phys. A*, **122**(9), 792.

Ebrahimi, F. and Barati, M.R. (2016j), "A nonlocal higher-order refined magneto-electro-viscoelastic beam model for dynamic analysis of smart nanostructures", *Int. J. Eng. Sci*., **107**, 183-196.

Ebrahimi, F. and Barati, M.R. (2016k), "Hygrothermal effects on vibration characteristics of viscoelastic FG nanobeams based on nonlocal strain gradient theory", *Compos. Struct*., **159**, 433-444.

Ebrahimi, F. and Barati, M.R. (2016l), "Buckling analysis of nonlocal third-order shear deformable functionally graded piezoelectric nanobeams embedded in elastic medium", *J. Brazilian Soc. Mech. Sci. Eng*., 1-16.

Ebrahimi, F. and Barati, M.R. (2016m), "Magnetic field effects on buckling behavior of smart size-dependent graded nanoscale beams", *Eur. Phys. J. Plus*, **131**(7), 1-14.

Ebrahimi, F. and Barati, M.R. (2016n), "Buckling analysis of smart size-dependent higher order magneto-electro-thermo-elastic functionally graded nanosize beams", *J. Mechanics*, 1-11.

Faingold, A., Cohen, S.R., Reznikov, N. and Wagner, H.D. (2013), "Osteonal lamellae elementary units: Lamellar microstructure, curvature and mechanical properties", *Acta Biomaterialia*, **9**(4), 5956-5962.

Gourion-Arsiquaud, S., Marcott, C., Hu, Q.and Boskey, A.L. (2014), "Studying variations in bone composition at nano-scale resolution: A preliminary report", *Calcif Tissue Int*., **95**(5), 413-418.

Hamed, E., Jasiuk, I., Yoo, A., Lee, Y.H. and Liszka, T. (2012), "Multi-scale modelling of elastic moduli of trabecular bone", *J. R. Soc.*, **9**, 1654-1673.

Hamed, E., Lee, Y.H. and Jasiuk, I. (2010), "Multiscale modeling of elastic properties of cortical bone", *Acta Mechanica*, **213**, 131-154.

Hamza-Cherif, R., *et al*. (2018), "Vibration analysis of nano beam using differential transform method including thermal effect", *J. Nano Res.*, **54**, 1-14.

Hassenkam, T., Fantner, G.E., Cutroni, J.A., Weaver, J.C., Morse, D.E. and Hansma, P.K. (2004), "High-resolution AFM imaging of intact and fractured trabecular bone", *Bone*, **35**, 4-10.

Hoffler, C.E., Moore, K.E., Kozloff, K., Zysset, P.K., Brown, M.B. and Goldstein, S.A. (2000), "Heterogeneity of bone lamellar-level elastic moduli", *Bone*, **26**(6), 603- 609.

Karami, B., *et al.* (2018), "Nonlocal strain gradient 3D elasticity theory for anisotropic spherical nanoparticles", *Steel Compos. Struct.*, **27**(2), 201-216.

Lim, C.W., Zhang, G. and Reddy, J.N. (2015), "A higher-order nonlocal elasticity and strain gradient theory and its applications in wave propagation", *J. Mech. Phys. Solids*, **78**, 298–313.

Liu, D., Weiner, S. and Wagner, H.D. (1999), "Anisotropic mechanical properties of lamellar bone using miniature cantilever bending specimens", *J. Biomechanics*, **32**, 647-654.

Mercan, K. and Civalek, O. (2016), "DSC method for buckling analysis of boron nitride nanotube (BNNT) surrounded by an elastic matrix", *Compos. Struct*., **143**, 300-309.

Mitchell, J. and Van Heteren, A.H. (2015), "A literature review of the spatial organization bone of lamellar", *Comptes Rendus Palevol*, **45**(5), 1219-1226.

Mokhtari, F. and Beni, Y.T. (2016), "Free vibration analysis of microtubules as orthotropic elastic shells using stress and strain gradient elasticity theory", *J. Solid Mech*., **8**(3), 511-529.

Mokhtar, Y., *et al.* (2018), "A novel shear deformation theory for buckling analysis of single layer graphene sheet based on nonlocal elasticity theory", *Smart Struct. Syst.*, **21**(4), 397-405.

Mouffoki, A., *et al.* (2017), "Vibration analysis of nonlocal advanced nanobeams in hygro-thermal environment using a new two-unknown trigonometric shear deformation beam theory", *Smart Struct. Syst.*, **20**(3), 369-383.

Qian, X.S., Zhang, J.Q. and Ru, C.Q. (2007), "Wave propagation in orthotropic microtubules", *J. Appl. Phys*., **101**(8), 84702.

Ren, L., Yang, P., Wang, Z., Zhang, J., Ding, C. and Shang, P. (2015), "Biomechanical and biophysical environment of bone from the macroscopic to the pericellular and molecular level", *J. Mech. Behavior of Biomedical Mater*., **50**, 104-122.

Rho, J.Y., Liisa, K.S. and Peter, Z. (1998), "Mechanical properties and the hierarchical structure of bone", *Medical Eng. Phys*., **20**, 92-102.

Shaat, M. (2018), "A reduced micromorphic model for multiscale materials and its applications in wave propagation", *Compos. Struct*., **201**, 446-454.

Sun, X., Zhao, H., Yu, Y., Zhang, S., Ma, Z., Li, N., Yu, M. and Hou, P. (2016), "Variations of mechanical property of out circumferential lamellae in cortical bone along the radial by nanoindentation", *Aip Adv*., **6**, 115116-1–10.

Tanaka, Y. (2018), "Active vibration compensator on moving vessel by hydraulic parallel mechanism", *Int. J. Hydromechatronics*, **1**(3), 350-359.

Tlidji, Y., *et al.* (2019), "Vibration analysis of different material distributions of functionally graded microbeam", *Struct. Eng. Mech.*, **69**(6), 637-649.

Unal, M., Cingoz, F., Bagcioglu, C., Sozer, Y. and Akkus, O. (2018), "Interrelationships between electrical,

mechanical and hydration properties of cortical bone”, *J. Mech. Behav. Biomed.Mater.*, **7**, 12-23.
Wang, Z., Xie, Z. and Huang, W. (2018), “A pin-moment model of flexoelectric actuators”, *Int. J. Hydromechatronics*, **1**(1), 72-90.
Weiner, Steve, Traub Wolfie, and H. Daniel Wagner. (1999), “Lamellar bone: Structure–function relations”, *J. Struct. Biology*, **126**, 241-255.
Xie, S., Manda, K., Wallace, R.J., Levrero-Florencio, F., Simpson, A.H.R. and Pankaj, P. (2017), “Time dependent behaviour of trabecular bone at multiple load levels”, *Ann.Biomed. Eng.*, **45**(5), 1219-1226.
Yazid, M., *et al.* (2018), “A novel nonlocal refined plate theory for stability response of orthotropic single-layer graphene sheet resting on elastic medium”, *Smart Struct. Syst.*, **21**(1), 15-25.
Youcef, D.O., *et al.* (2018), “Dynamic analysis of nanoscale beams including surface stress effects”, *Smart Struct. Syst.*, **21**(1), 65-74.
Zemri, A., *et al*. (2015), “A mechanical response of functionally graded nanoscale beam: an assessment of a refined nonlocal shear deformation theory beam theory”, *Struct. Eng. Mech.*, **54**(4), 693-710.

CC